Propagation in Dielectric Slab Loaded Rectangular Waveguide*

P. H. VARTANIAN†, W. P. AYRES†, AND A. L. HELGESSON‡

Summary—**Propagation in dielectric loaded rectangular waveguide is investigated theoretically for varying slab thickness and dielectric constant. The slabs are placed across the center of the waveguide in the *E* plane. This geometry is found to offer bandwidths in excess of double that of rectangular waveguide for dielectrics having dielectric constants of approximately 18. Power handling capacities which are double or triple that of standard waveguide are achievable using the dielectric loaded waveguide. In addition to the theory, design curves of bandwidth, guide wavelength, cutoff wavelength, impedance, power handling capacity, wall losses, and dielectric losses are presented and compared to experiment where possible.**

List of Symbols

$k = \omega/c = \omega\sqrt{\mu_0\epsilon_0} = 2\pi/\lambda_0$.
$k_c = 2\pi/\lambda_c$.
$\beta = 2\pi/\lambda_g$.
λ_0 = free-space wavelength.
λ_g = guide wavelength.
λ_c = guide cutoff wavelength.
μ_0 = free-space permeability.
ϵ_0 = free space permittivity.
$\epsilon = \mathcal{E}\epsilon_0$ = complex permittivity.
$= \epsilon_0 (\mathcal{E}' - j\mathcal{E}'')$
$\mathcal{E}'$ = relative dielectric constant.
$\mathcal{E}''$ = loss factor.
$\tan\delta = \mathcal{E}''/\mathcal{E}'$ = loss tangent.
$\eta = \sqrt{\mu_0/\epsilon_0} = 377$ ohms.
$r = s/d = (c/a)/(1 - c/a)$.

Introduction

WITH the development of low-loss, high-dielectric constant materials, a new type of waveguide transmission line offers advantages in bandwidth and power handling capacity over conventional waveguides. The geometry to be considered is a rectangular waveguide loaded with a dielectric slab placed across the center of the waveguide in the *E* plane. That this geometry would broad band the rectangular waveguide is readily apparent by comparison with the ridged waveguide. Both the ridged and the dielectric loaded waveguides add capacitance to the dominant mode, while only slightly affecting the capacitance associated with the next higher mode. The dielectric loaded waveguide, unlike the ridged guide, does not reduce the air gap and, consequently, the power handling capacity, but instead adds material having a higher breakdown strength to the region where breakdown is most likely. Consequently, the power handling capacity is higher with the loaded waveguide. The general results, if compared to ridged waveguide, are that the dielectric loaded waveguide is superior in every respect, with the assumption that suitably low-loss dielectric materials are available.

This work theoretically investigates the propagation characteristics of the TE_{no} modes in dielectric loaded waveguide. The analysis yields design curves of bandwidth, guide wavelength, cutoff wavelength, impedance, power handling capacity, wall losses, and dielectric losses. Previous treatments of dielectric loaded rectangular waveguide have considered the cutoff relations[1] and other loading geometries.[2] Berk,[3] by variational methods, has derived approximate relations for the guide wavelength.

General Theory

The geometry of the dielectric slab loaded waveguide is shown in Fig. 1. It consists of a dielectric slab mounted in the *E* plane at the center of a rectangular waveguide.

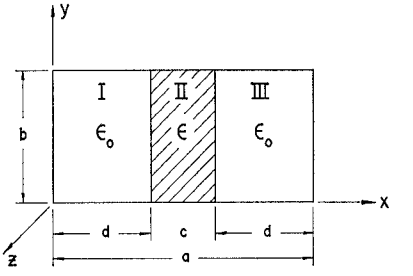

Fig. 1—Dielectric loaded waveguide geometry.

The two types of modes corresponding to TE and TM modes are called the longitudinal section electric (LSE) and longitudinal section magnetic (LSM) modes. The LSE mode is characterized by $E_x = 0$ and the LSM mode by $H_x = 0$. Considerations of the boundary conditions lead to the fact that for modes having no *y* dependence

* Manuscript received by the PGMTT, October 4, 1957; revised manuscript received, December 6, 1957. This work was performed at the Microwave Physics Lab., Sylvania Elec. Products, Inc., and was sponsored in part by the U. S. Army Signal Corps under Contract No. DA 36-039-SC-73188.

† Microwave Eng. Labs., Inc., Palo Alto, Calif.; formerly with Sylvania Microwave Phys. Lab., Mountain View, Calif.

‡ Massachusetts Institute of Technology, Cambridge, Mass., on educational leave from Sylvania Microwave Phys. Lab., Mountain View, Calif.

[1] C. Montgomery, R. Dicke, and E. Purcell, "Principles of Microwave Circuits," McGraw-Hill Book, Co., Inc., New York, N. Y., Rad. Lab. Ser., vol. 8, pp. 386–387; 1948. This work appears to have typographical errors in several of the equations. The curves, however, are correct at the calculated points.

[2] L. Pincherle, "Electromagnetic waves in metal tubes filled longitudinally with two dielectrics," *Phys. Rev.*, vol. 66, pp. 118–130; September, 1944.

[3] A. D. Berk, "Variational principles for electromagnetic resonators and waveguides," IRE TRANS., vol. AP-4, pp. 104–111; April, 1956.

of fields, the LSE mode is a TE mode (*i.e.*, E_z is zero). Thus, for these modes with propagation according to $\exp j(\omega t-\beta z)$, Maxwell's equations give the following relations:

$$E_y = -\frac{\omega\mu_0}{\beta} H_x \tag{1}$$

$$\frac{\partial E_y}{\partial x} = -j\omega\mu_0 H_z \tag{2}$$

$$\frac{\partial H_z}{\partial x} + j\beta H_x + j\omega\epsilon E_y = 0. \tag{3}$$

From (1) through (3), it can be shown that

$$\frac{\partial^2 H_z}{\partial x^2} + (\mathcal{E}k^2 - \beta^2)H_z = 0 \tag{4}$$

where $\epsilon = \mathcal{E}\epsilon_0$ is the dielectric constant in the region under consideration and $k^2 = \omega^2\epsilon_0\mu_0$, the square of the free-space wave number. Since we have assumed modes having fields which are independent of y, let

$$H_z = Ag(x)e^{j(\omega t-\beta z)} \tag{5}$$

and from (1) and (3)

$$E_y = j\omega\mu_0 \frac{\partial H_z}{\partial x} \begin{cases} \dfrac{1}{k^2 - \beta^2} & \text{in I} \\ \dfrac{1}{\mathcal{E}k^2 - \beta^2} & \text{in II} \\ \dfrac{1}{k^2 - \beta^2} & \text{in III.} \end{cases} \tag{6}$$

For the purpose of analysis, the TE modes are separated into $TE_{odd,0}$ and $TE_{even,0}$ modes. For the $TE_{odd,0}$ modes, $g(x)$ is an antisymmetric function about the center of the guide. Hence, let

$$g(x) = \begin{cases} \cos\dfrac{px}{d} & \text{in I} \\ B\sin\dfrac{q}{s}\left(\dfrac{a}{2} - x\right) & \text{in II} \\ -\cos\dfrac{p}{d}(a - x) & \text{in III} \end{cases} \tag{7}$$

where p and q are unknowns and $s = c/2$. From (4), (and for all TE modes),

$$\left(\frac{p}{d}\right)^2 = k^2 - \beta^2 \tag{8}$$

$$\left(\frac{q}{s}\right)^2 = \mathcal{E}k^2 - \beta^2. \tag{9}$$

The boundary conditions that H_z and E_y be continuous require

$$B = \frac{\cos p}{\sin q} \tag{10}$$

$$\frac{\tan p}{p} = r\frac{\cot q}{q} \tag{11}$$

where

$$r = \frac{s}{d} = \frac{c/a}{1 - c/a}.$$

The limits on p and q for the TE_{no} modes (n odd) are

$$0 \le q \le \frac{n\pi}{2}$$

$$-\infty \le p^2 \le \left(\frac{n\pi}{2}\right)^2. \tag{12}$$

Eliminating β from (8) and (9), there results

$$q^2 = r^2p^2 + \frac{(\mathcal{E} - 1)}{4}\left(\frac{rka}{1 + r}\right)^2 \tag{13}$$

which along with (11) and (12) permits finding p and q.

As a function of slab thickness, q^2 is zero for zero slab thickness and increases monotonically to $(n\pi/2)^2$ for increasing slab thickness. The quantity p^2, on the other hand, is $(n\pi/2)^2$ for zero slab thickness. As the slab is increased in width, p^2 decreases to a negative minimum returning asymptotic to zero for a dielectric filled guide. The negative values of p^2 indicate that the fields are experiencing exponential decay outside the slab. For such values of p^2, it would be imagined that the metallic walls at $x = 0$ and $x = a$ could be removed with little effect on the propagation characteristics. This has been experimentally verified for a slab of $\mathcal{E} = 9$. Curves showing the transverse electric field as a function of frequency are shown in Fig. 2. It is seen that for frequencies

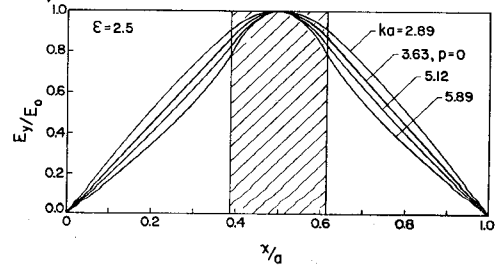

Fig. 2—Electric fields in dielectric loaded waveguide for several frequencies.

and slab thicknesses producing large negative values of p^2, the energy is highly concentrated in the dielectric slab. The $p^2 = 0$ condition is of interest since the electric field in the air space has a constant gradient. For $ka = 3.63$, the fields are linear in the air space. For a higher frequency, the fields decay exponentially in the air spaces.

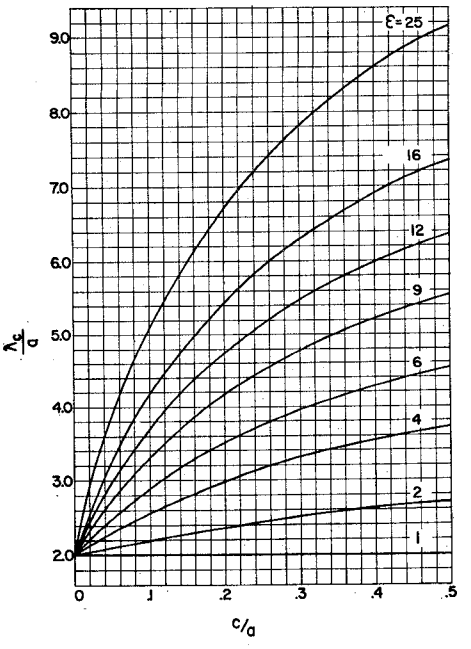

Fig. 3—Cutoff wavelength for the TE_{10} mode.

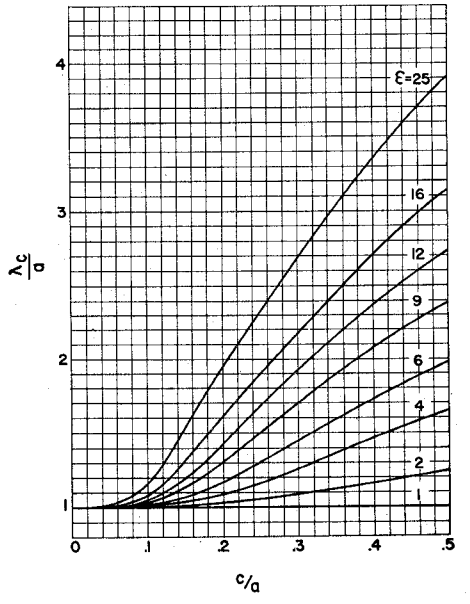

Fig. 4—Cutoff wavelength for the TE_{20} mode.

Propagation Characteristics

The cutoff frequency relations are easily found by setting $\beta=0$ in (8), (9), and (11). This leads to the equation for cutoff for the $TE_{odd,0}$ modes

$$\tan\frac{k_c a}{2(1+r)}=\frac{1}{\sqrt{\varepsilon}}\cot\frac{\sqrt{\varepsilon}k_c a r}{2(1+r)} \tag{14}$$

where

$$k_c=\frac{2\pi f_{cutoff}}{c}.$$

Similarly, it can be shown that for the $TE_{even,0}$ modes that

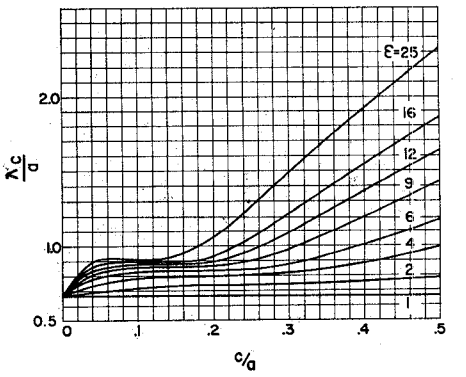

Fig. 5—Cutoff wavelength for the TE_{30} mode.

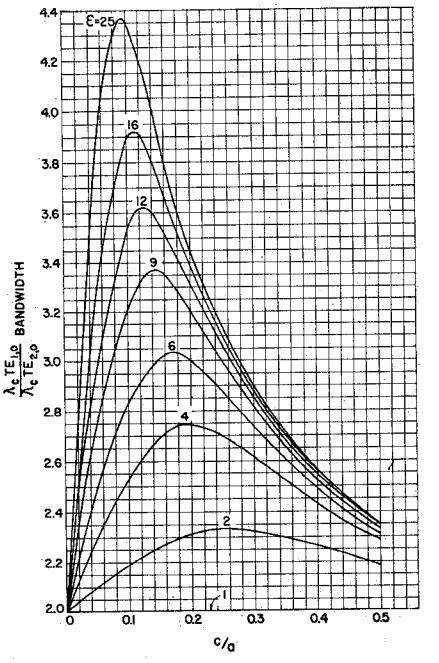

Fig. 6—Bandwidth defined on the basis of the ratios of cutoff wavelengths for the TE_{10} and TE_{20} modes.

$$\tan\frac{k_c a}{2(1+r)}=-\frac{1}{\sqrt{\varepsilon}}\tan\frac{\sqrt{\varepsilon}rk_c a}{2(1+r)}. \tag{15}$$

The normalized cutoff wavelengths calculated from (14) and (15) for the TE_{10}, TE_{20}, and TE_{30} modes are shown in Fig. 3 through Fig. 5 as a function of slab thickness and dielectric constant. The bandwidth, defined as the ratio of the cutoff wavelength for the TE_{10} mode to the cutoff wavelength for the TE_{20} mode is shown in Fig. 6. It is shown that for each dielectric constant there is a slab thickness which gives maximum bandwidth. This slab thickness, called the optimum slab thickness, and the associated maximum bandwidth are plotted in Fig. 7. It is seen that a slab of dielectric constant 18.1 can *double* the bandwidth of air filled waveguide. A dielectric constant of 9 gives a 1.68 improvement in bandwidth.

For the TE_{10} mode, the ka vs βa plot is calculated from (11) and (13). The quantities ka and βa are the reciprocals of the free space and guided wavelengths

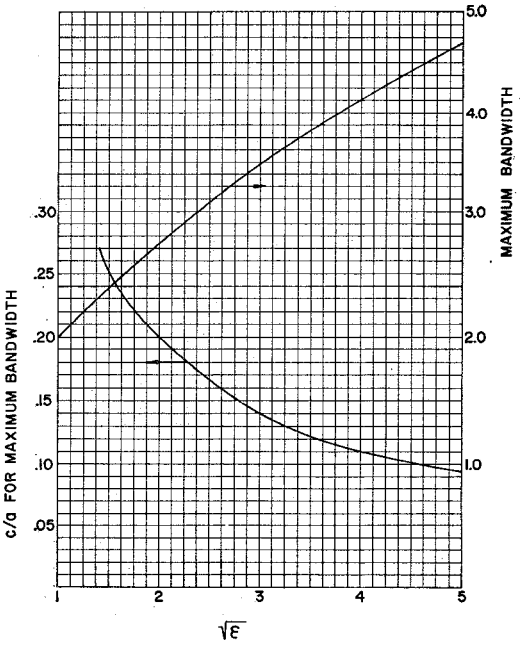

Fig. 7—Maximum bandwidth achievable for a given dielectric constant and the dielectric thickness which gives this maximum bandwidth.

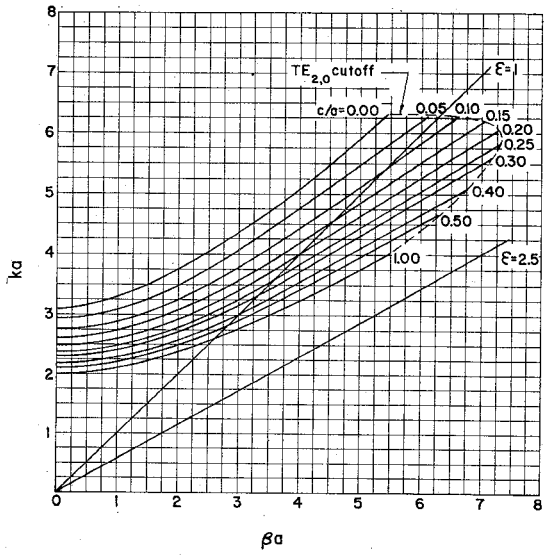

Fig. 8—ka vs βa plot for $\varepsilon = 2.5$.

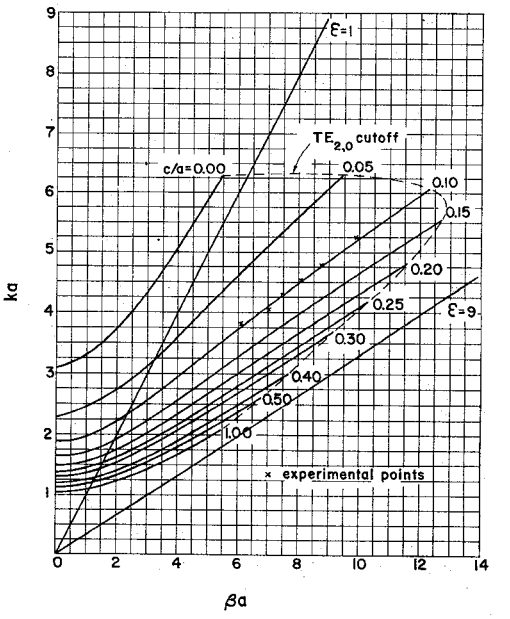

Fig. 9—ka vs βa plot for $\varepsilon = 9$. Experimental points taken in X-band waveguide are shown.

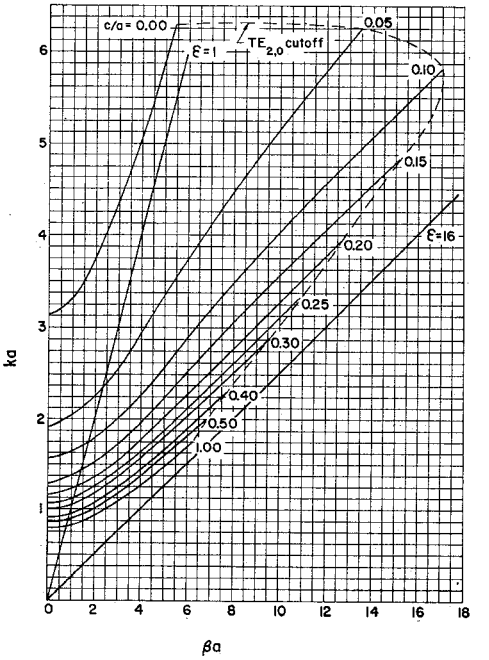

Fig. 10–ka vs βa plot for $\varepsilon = 16$.

normalized to the waveguide width. Fig. 8 through Fig. 10 are the results for dielectric constants of 2.5, 9, and 16.[4] Asymptotes for $ka = \beta a$ and $ka = \beta a/\sqrt{\varepsilon}$ also are shown. For sufficiently high frequency, the curves are all asymptotic to $ka = \beta a/\sqrt{\varepsilon}$. The $c/a = 0$ curve is, of course, asymptotic to $ka = \beta a$. From (8) it can be shown that

$$\frac{\lambda_g}{\lambda_0} = \left\{1 - \left[\frac{2p(1+r)}{ka}\right]^2\right\}^{-1/2}, \qquad (16)$$

where λ_g and λ_0 are the guide and free-space wavelengths. This shows that for frequencies and geometries where $2p(1+r) < ka$, the guide and free-space wavelengths are approximately equal. This also shows that the points where $p^2 = 0$ lie on the $ka = \beta a$ line in Fig. 8 through Fig. 10.

Experimental points are shown on the $\varepsilon = 9$ curve and show very good agreement with the theory. These measurements were made in X-band waveguide. It is interesting to note in passing that this X-band waveguide with a dielectric slab 0.126-inch thick has upper and lower frequency cutoffs of 11.93 and 3.54 kmc.

The slope of the line from the origin to points on the

[4] These dielectric constants were chosen to give a range of data which would be useful for commonly used low-loss dielectrics. These materials are available in the form of titanium dioxide loaded polystyrene ($\varepsilon = 2.5$ to 25).

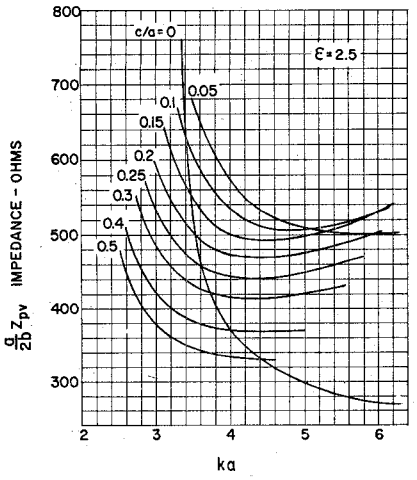

Fig. 11—Normalized power voltage impedance for $\varepsilon = 2.5$.

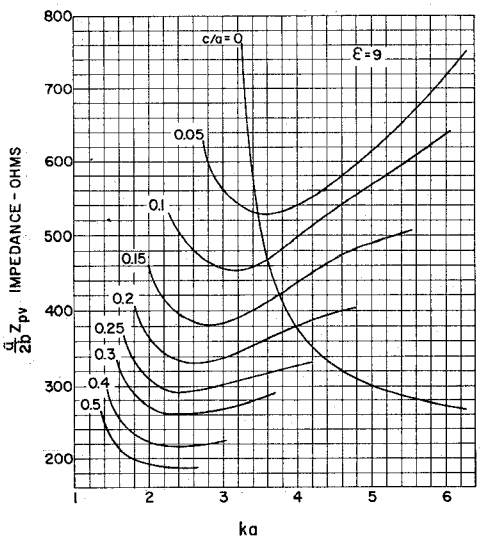

Fig. 12—Normalized power voltage impedance for $\varepsilon = 9$.

ka vs βa plot gives the group velocity of the structure. It is seen that over certain frequency ranges the dielectric loading can give a relatively constant group velocity. As such, this type waveguide could be useful in devices requiring a slow wave structure.

Impedance

The wave impedance defined by

$$Z_0 = \frac{E_y}{H_x} = \eta \frac{ka}{\beta a}$$

where $\eta = 377$ ohms can easily be found from the ka vs βa curves.

The power-voltage impedance can be defined by

$$Z_{PV} = \frac{VV^*}{2P}$$

where P is the power carried by the guide and V is the voltage across the center of the guide. From (6)

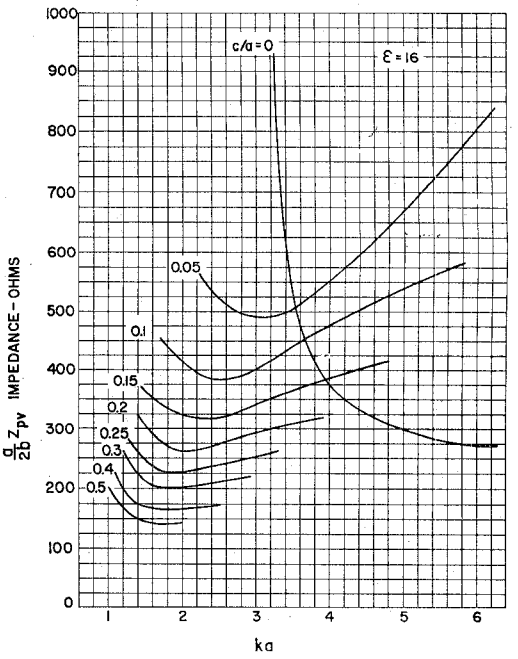

Fig. 13—Normalized power voltage impedance for $\varepsilon = 16$.

$$E_y = \begin{cases} E_0 \dfrac{\cos q}{\sin p} \sin \dfrac{px}{d} \\ E_0 \cos \dfrac{q}{s}\left(\dfrac{a}{2} - x\right) \\ E_0 \dfrac{\cos q}{\sin p} \sin \dfrac{p}{d}(a - x) \end{cases} \tag{17}$$

where

$$E_0 = -\frac{j\omega\mu_0 A p \sin p}{(k^2 - \beta^2) d \cos q} = -\frac{j\omega\mu_0 A B q}{(\varepsilon k^2 - \beta^2) s}.$$

The power in the waveguide is

$$P = -\frac{1}{2}\int E_y H_x^* dx dy = \frac{E_0^2 abR}{4Z_0(1 + r)} \tag{18}$$

where

$$R = r\left(1 + \frac{\sin 2q}{2q}\right) + \left(\frac{\cos q}{\sin p}\right)^2\left(1 - \frac{\sin 2p}{2p}\right).$$

Hence, from (18)

$$Z_{PV} = \frac{2\eta(1 + r)}{R} \frac{b}{a} \frac{ka}{\beta a}. \tag{19}$$

This impedance has been calculated and is plotted for $\varepsilon = 2.5$, 9, and 16 in Fig. 11 through Fig. 13.

Power Handling Capacity

The power handling capacity is calculated from (17) and (18). It is assumed that the waveguide will break down at the point of highest field in the air space. This point obviously is at the surface of the dielectric or at $x = d$. With this assumption

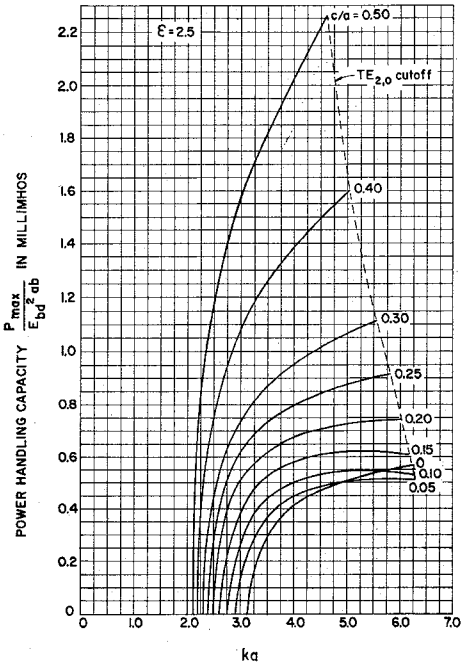

Fig. 14—Power handling capacity for $\varepsilon = 2.5$. The $c/a = 0$ curve represents unloaded waveguide.

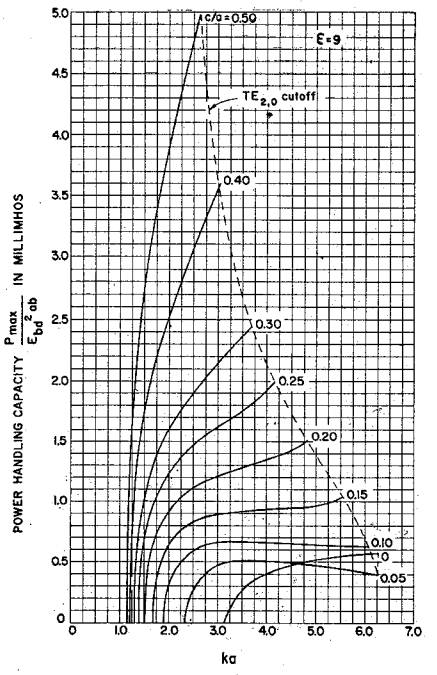

Fig. 15—Power handling capacity for $\varepsilon = 9$. The $c/a = 0$ curve represents unloaded waveguide.

$$P_{\max} = \frac{E_{bd}^2 abR}{4\eta(1 + r)\cos^2 q}\left(\frac{\beta a}{ka}\right) \tag{20}$$

where E_{bd} is the breakdown electric field in air. The quantity $P_{\max}/E_{bd}^2 ab$ is plotted as a function of frequency with slab thickness as a parameter for dielectric constants 2.5, 9, and 16 in Fig. 14 through Fig. 16. The $c/a = 0$ curves give the maximum power for the unloaded guide.

It is noted that for very thin slabs the power handling capacity is below that for the unloaded guide. This is because the energy is drawn toward the slab, but the slab is not thick enough to contain the region of high field. As the slab thickness is increased, the energy is further concentrated, but the high fields are now contained in the dielectric. Consequently, the power handling capacity exceeds that for the unloaded waveguide. For the $\varepsilon = 9$ case, for the slab thickness corresponding to maximum bandwidth, the power handling capacity is almost twice that for unloaded waveguide.

The assumption of breakdown at the dielectric surface fails when the field for breakdown in the dielectric becomes less than $E_{bd}/\cos q$. In this case, $E_{bd}/\cos q$ should be replaced by the breakdown electric field for the dielectric.

A practical problem in achieving high-power handling capability is the complete elimination of air gaps between the dielectric slab and the waveguide. A small air gap is equivalent to a small capacity in series with a large capacity (the dielectric slab) and breakdown is very likely across this small gap. As seen from Fig. 14 through Fig. 16, the power handling capacity of the loaded waveguide can be considerably in excess of the unloaded waveguide. In general, transforming sections from unloaded to loaded waveguide (especially those utilizing thin slab matching sections) will limit the power handling ability of the transmission line.

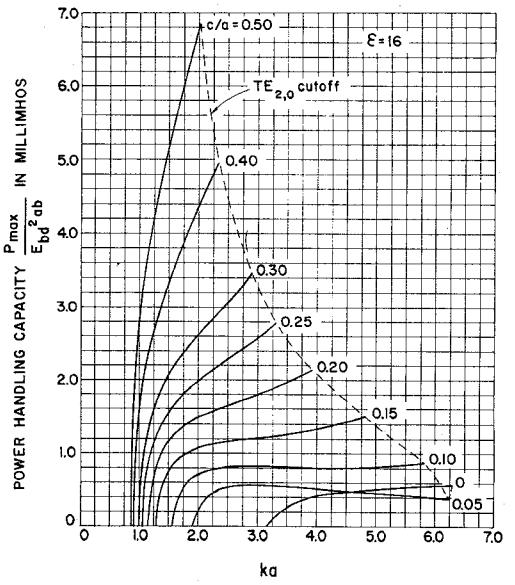

Fig. 16—Power handling capacity for $\varepsilon = 16$. The $c/a = 0$ curve represents unloaded waveguide.

Waveguide Losses

Since the magnetic fields are being concentrated about the slab, it might be expected that the waveguide wall losses might be considerably increased by the addition of the dielectric slab. In general, while the losses are increased, the increase is not significant. The power dissipated in the waveguide walls is

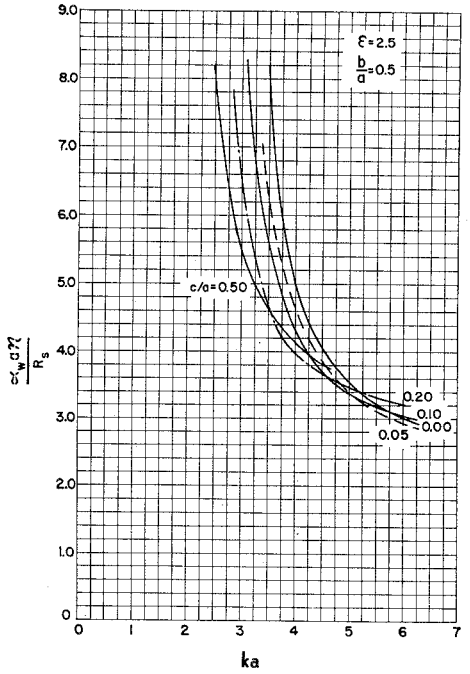

Fig. 17—Wall losses in dielectric loaded waveguide for $\mathcal{E}=2.5$.

$$P_w = \frac{R_s}{2}\int |H_t|^2 dS$$

where R_s is the surface resistivity of the metal waveguide walls and H_t is the magnetic field tangential to the waveguide wall. Here as usual it is assumed that the loss free H_t is a good approximation to the actual H_t. The attenuation per unit length due to wall losses is

$$\alpha_w = \frac{P_w}{2P}.$$

Performing the indicated integrations and substituting from (1), (5), (17), and (18), we find

$$\frac{\alpha_w a\eta}{R_s} = \left(\frac{\beta a}{ka}\right)\left(\frac{a}{b}\right)\left\{\left[\left(\frac{ka}{\beta a}\right)^2 - 1\right]\cdot\left[R' + 2(1+r)\frac{b}{a}\left(\frac{\cos q}{\sin p}\right)^2\right]\frac{1}{R} + 1\right\} \quad (21)$$

where

$$R' = \left(\frac{\cos q}{\sin p}\right)^2\left(1 + \frac{\sin 2p}{2p}\right) + \left(\frac{q}{p}\right)^2\frac{1}{r}\left(1 - \frac{\sin 2q}{2q}\right).$$

These waveguide losses are plotted in Fig. 17 through Fig. 19 for dielectric constants of 2.5, 9, and 16. The aspect ratio has been chosen to be 2:1. The losses are found to be comparable in magnitude to the unloaded waveguide losses except for effects connected with the lowering of the low-frequency cutoff by the dielectric addition. An interesting point is seen where the addition of a dielectric slab actually reduces the waveguide losses. This is because the low-frequency cutoff is reduced, thus reducing the transverse currents in the waveguide and consequently reducing the waveguide losses.

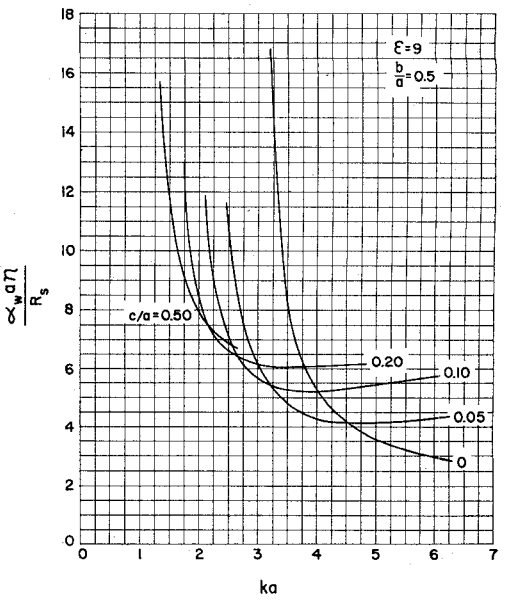

Fig. 18—Wall losses in dielectric loaded waveguide for $\mathcal{E}=9$.

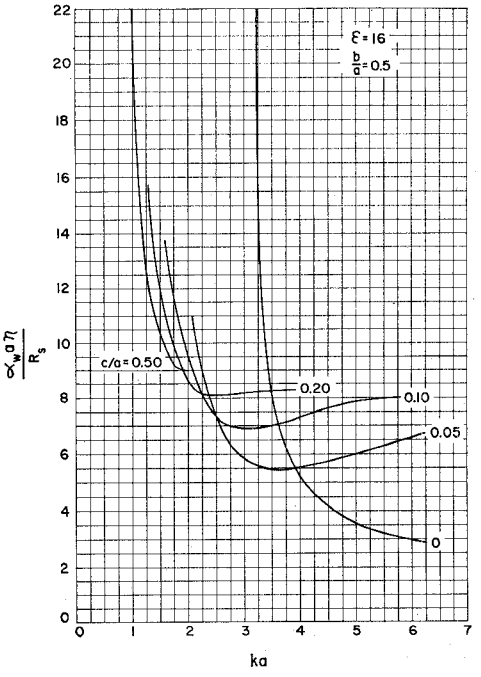

Fig. 19—Wall losses in dielectric loaded waveguide for $\mathcal{E}=16$.

Dielectric Losses

Dielectric losses are calculated from

$$P_d = 2\int_d^{a/2}\int_0^b \frac{|E_y|\,|J_y|}{2}dxdy = \sigma\int_d^{a/2}\int_0^b |E_y|^2 dxdy,$$

$$\sigma = \omega\mathcal{E}''\epsilon_0, \qquad \alpha_d = \frac{P_d}{2P}.$$

Performing the indicated integration, and substituting from (17) and (18), the dielectric loss in found to be given by

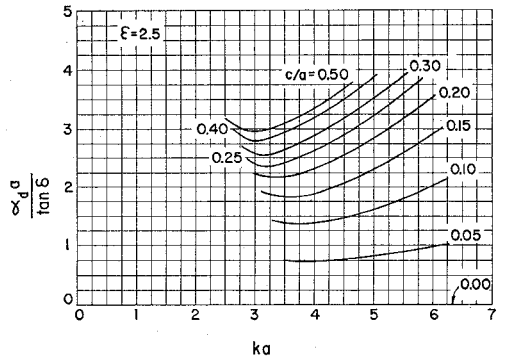

Fig. 20—Dielectric losses for $\varepsilon = 2.5$.

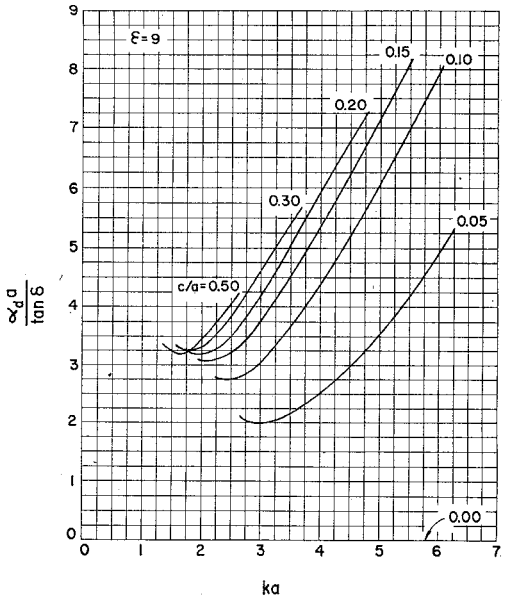

Fig. 21—Dielectric losses for $\varepsilon = 9$.

$$\frac{\alpha_d a}{\tan\delta} = \frac{\varepsilon' ka}{2}\left(\frac{ka}{\beta a}\right)\frac{r\left(1+\dfrac{\sin 2q}{2q}\right)}{R}. \qquad (22)$$

Plots of dielectric loss as a function of frequency with slab thickness as a parameter are shown in Fig. 20 through Fig. 22. It is apparent that, as might be expected, losses are highest for thick slabs and high frequencies. For a typical dielectric with $\varepsilon' = 9$, $\varepsilon'' = 0.005$, the loss per meter in X-band waveguide with $c/a = 0.15$ and $ka = 4.0$ is approximately 1.1 db/meter.

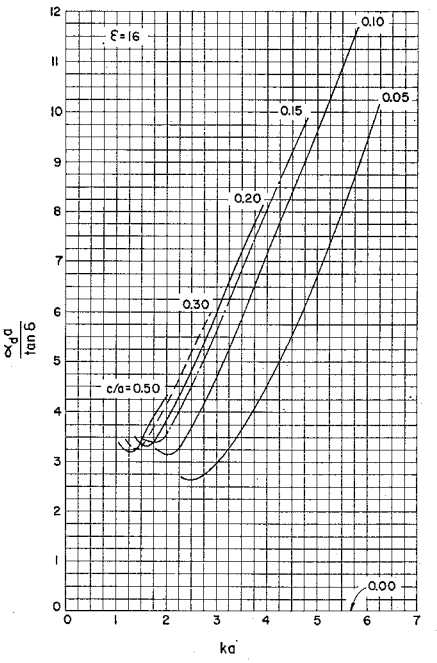

Fig. 22—Dielectric losses for $\varepsilon = 16$.

Conclusion

Dielectric slab loaded rectangular waveguide can afford significant advantage in bandwidth and power handling capacity over unloaded rectangular waveguide. It has been shown that by proper choice of dimensions and dielectrics, the bandwidth and power handling capacity can be significantly increased. The waveguide wall losses were found to be larger than, but still comparable to, those of unloaded waveguide. Finally, low-dielectric loss materials should permit reasonably low-loss transmission properties.

Acknowledgment

The authors are indebted to Mrs. R. Farrand for many of the numerical calculations.